Retrieval of vegetation variables using hyperspectral imagery of different spatial resolution

Sebastian Preidl
Daniel Doktor
Gundula Schulz
Steffen Lehmann
Gudrun Schuhmann

EnMAP-Workshop Bonn-Oberkassel
14.11.2013

HELMHOLTZ
CENTRE FOR
ENVIRONMENTAL
RESEARCH – UFZ

Introduction

- **Main objective:** Estimating biophysical crop variables (leaf chlorophyll content (LCC), leaf area index (LAI)) using hyperspectral images of different spatial resolution.
- **Research question:** With respect to the lower ground resolution of the upcoming EnMAP satellite sensor: How does spatial resolution effect the estimation of biophysical variables?
- **Approach:** Inversion of a radiative transfer model based on airborne hyperspectral data using a machine learning technique. Development of a process chain with minimal user interference.

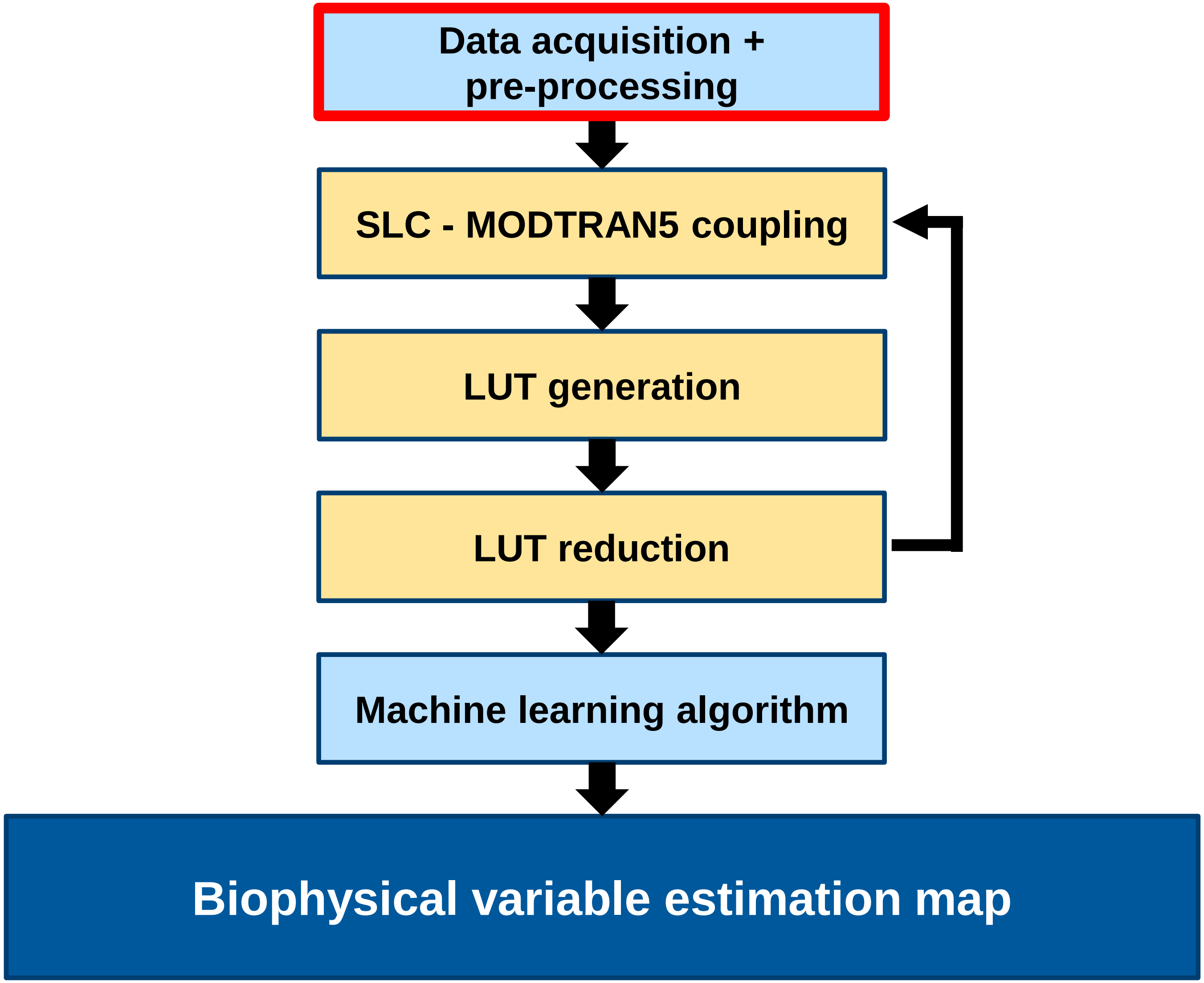
Data acquisition + pre-processing
SLC - MODTRAN5 coupling
LUT generation
LUT reduction
Machine learning algorithm
Biophysical variable estimation map

Data acquisition pre-processing → SLC - MODTRAN coupling → LUT generation → LUT reduction → Machine learning algorithm → Estimation map

EnMAP Hyperspectral Imager

2m3m

ASD FieldSpec3, SPAD Chlorophyll Meter, LI-COR 2000 ,
plant height, phenological stage

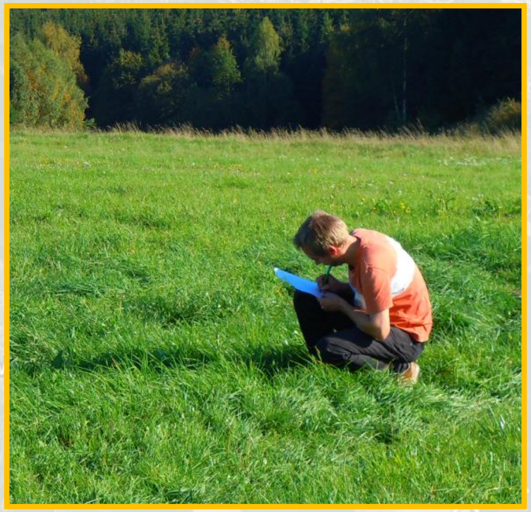

© 2013 Google
© 2009 GeoBasis-DE/BKG
Image © 2013 GeoBasis-DE/BKG

Pre-processing chain (in cooperation with GFZ)

Cal-file check: Wvl/FWHM correction

‚autodarkline' correction

DN-Values

radiometric correction (CaliGeo)

Resizing raw + radiance image

Radiance

destriping with ROME *

geometric correction (CaliGeo)

co-registration (DOP-Aufnahmen)

Mosaicking

Radiance-Mosaic

***** Rogaß, C.; Spengler, D.; Bochow, M.; Segl, K.; Lausch, A.; Doktor, D.; Roessner, S.; Behling, R.; Wetzel, H.-U.; Kaufmann, H. (2011): Reduction of Radiometric Miscalibration - Applications to Pushbroom Sensors. Sensors, 11, 6, 6370-6395.

The SLC and MODTRAN5 model were coupled* to build up a synthetic database of simulated vegetation radiances

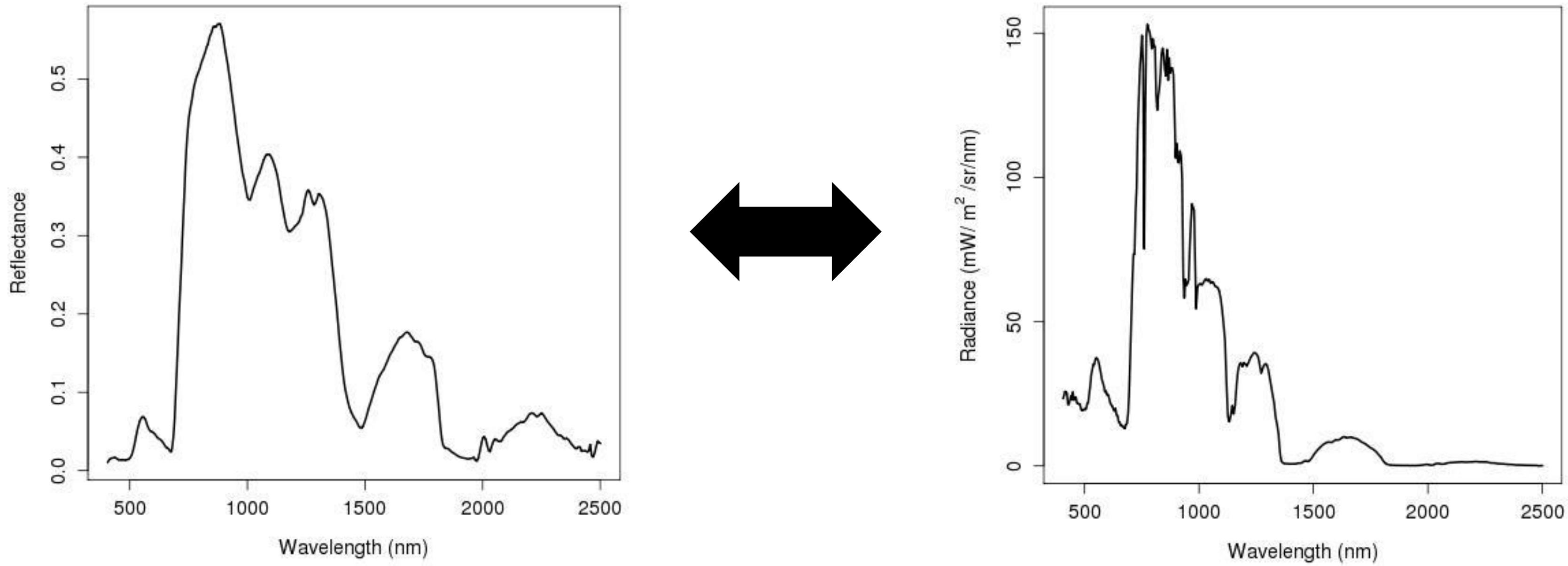

*W. Verhoef, B. Bach, „Simulation of hyperspectral and directional radiance images using coupled biophysical and atmospheric radiative transfer models," *Remote Sensing of Environment*, vol. 87, no. 1, pp. 23-41, 2003.

*V.C.E. Laurent, W. Verhoef, J.G.P.W. Clevers, et al., "Estimating forest variables from top-of-atmosphere radiance satellite measurements using coupled radiative transfer models," *Remote Sensing of Environment*, vol. 115, no. 4, pp. 1043-1052, 2011.

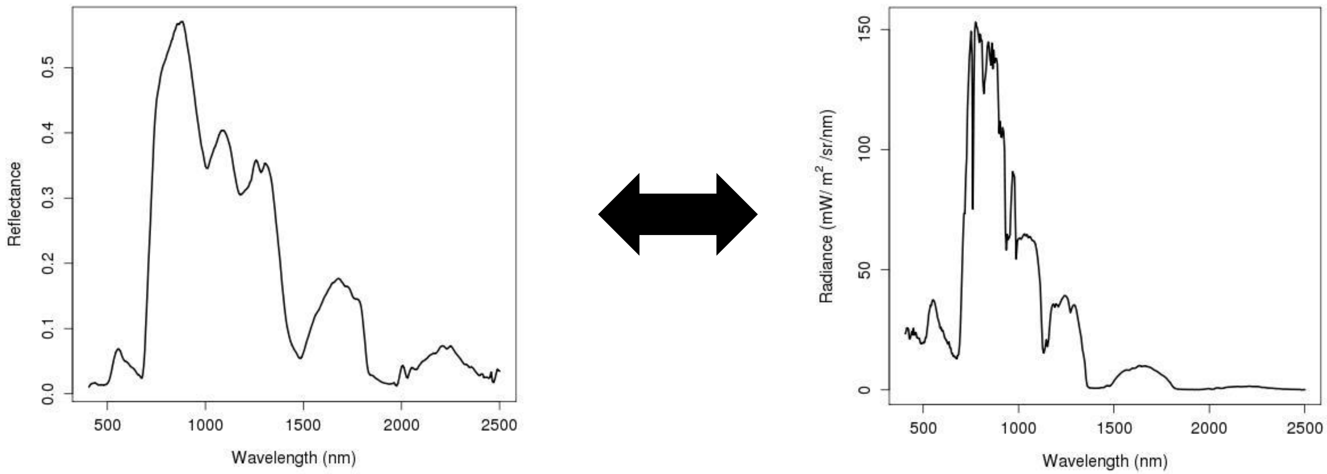

Advantage: - Reducing error propagation in the pre-processing chain:
⇨ No atmospheric correction of the AISA data
- Overcome sensor specific features in reflectance profiles

Without considering the adjacency effect at-sensor radiance (L_0) is calculated as:

$$L_o = \frac{E_s}{\pi} cos\theta_s \left(\rho_{so} + \frac{\tau_{ss} r_{sd} + \tau_{sd} r_{dd}}{1 - r_{dd}\rho_{dd}} \tau_{do} + \frac{\tau_{sd} + \tau_{ss} r_{sd}\rho_{dd}}{1 - r_{dd}\rho_{dd}} r_{do}\tau_{oo} + \tau_{ss} r_{so}\tau_{oo} \right)$$

Without considering the adjacency effect at-sensor radiance (L_0) is calculated as:

$$L_o = \frac{E_s}{\pi} cos\theta_s \left(\rho_{so} + \frac{\tau_{ss} r_{sd} + \tau_{sd} r_{dd}}{1 - r_{dd}\rho_{dd}} \tau_{do} + \frac{\tau_{sd} + \tau_{ss} r_{sd} \rho_{dd}}{1 - r_{dd}\rho_{dd}} r_{do} \tau_{oo} + \tau_{ss} r_{so} \tau_{oo} \right)$$

atmospheric parameters

surface reflectance factors

atmospheric parameters

MODTRAN output:	total path radiance, sunlight ground-reflected radiance, total ground-reflected radiance
3 MODTRAN runs:	surface albedos 0%, 50%, and 100%
MODTRAN ‘unknowns’:	H_2O, O_3, CO_2, aerosols, visibility

Simulating vegetation spectra using SLC*

surface reflectance factors

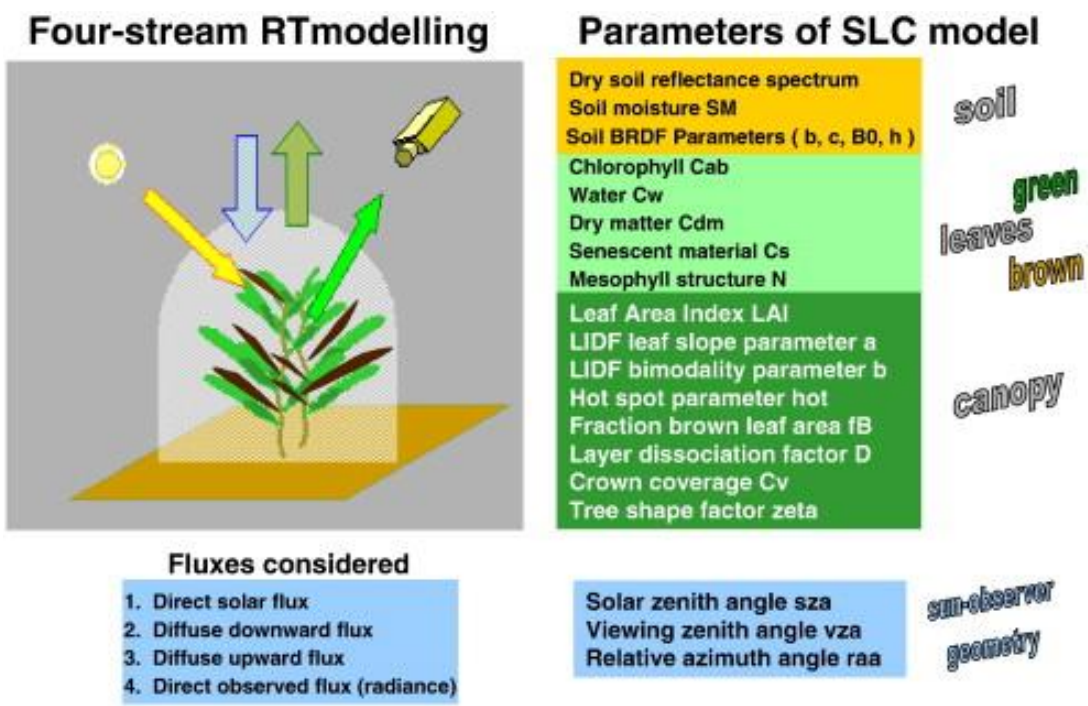

*W. Verhoef and H. Bach, ”Coupled soil–leaf-canopy and atmosphere radiative transfer modeling to simulate hyperspectral multi-angular surface reflectance and TOA radiance data,” *Remote Sensing of Environment*, vol. 109, pp. 166-182, 2007.

Picture: W. Verhoef and H. Bach, „ Simulation of Sentinel-3 images by four-stream surface–atmosphere radiative transfer modeling in the optical and thermal domains,” *Remote Sensing of Environment*, vol. 120, no. 2, pp. 197–207, 2012.

Data acquisition pre-processing → SLC - MODTRAN coupling → LUT generation → LUT reduction → Machine learning algorithm → Estimation map

EnMAP Hyperspectral Imager

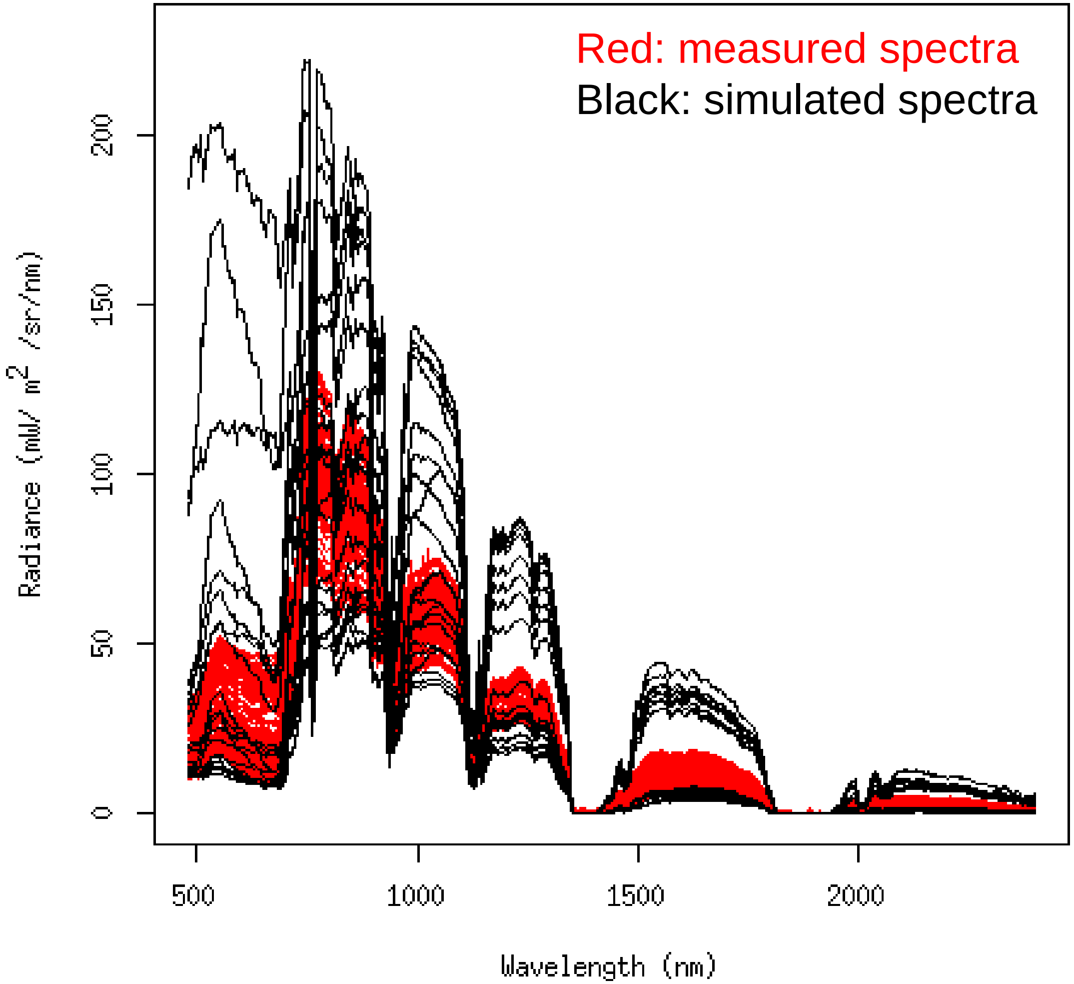

LUT reduction: using a singular value decomposition (SVD) of the correlation matrix of the measured and simulated spectral dataset

Objectives:

- Selecting spectra from the LUT showing highest similarity between measured and simulated dataset
- Supporting a faster and more precise inversion process

Approach:

- Projecting spectra in a higher dimensional space
- The eigenvalues (>1) determine the number of dimension to be considered
- Nearest neighbour algorithm is searching for the ‚best fit spectra'

Advantage:

- Fast even with a large LUTs

EnMAP Hyperspectral Imager

LUT reduction: using a singular value decomposition (SVD) of the correlation matrix of the measured and simulated spectral dataset

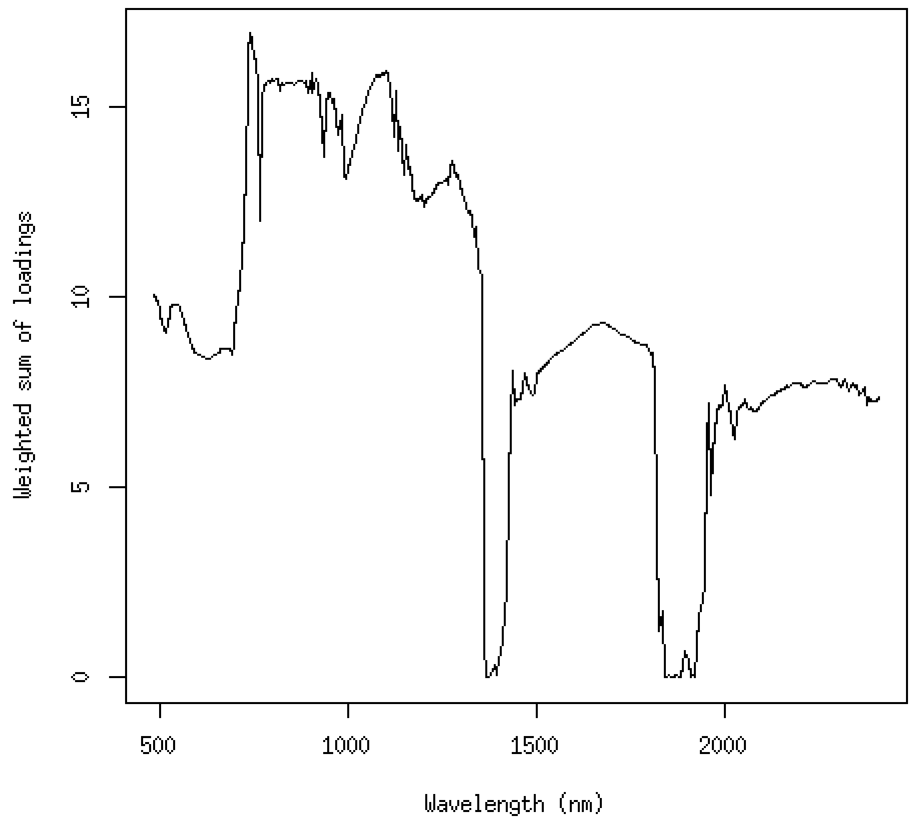

LUT reduction: using a singular value decomposition (SVD) of the correlation matrix of the measured and simulated spectral dataset

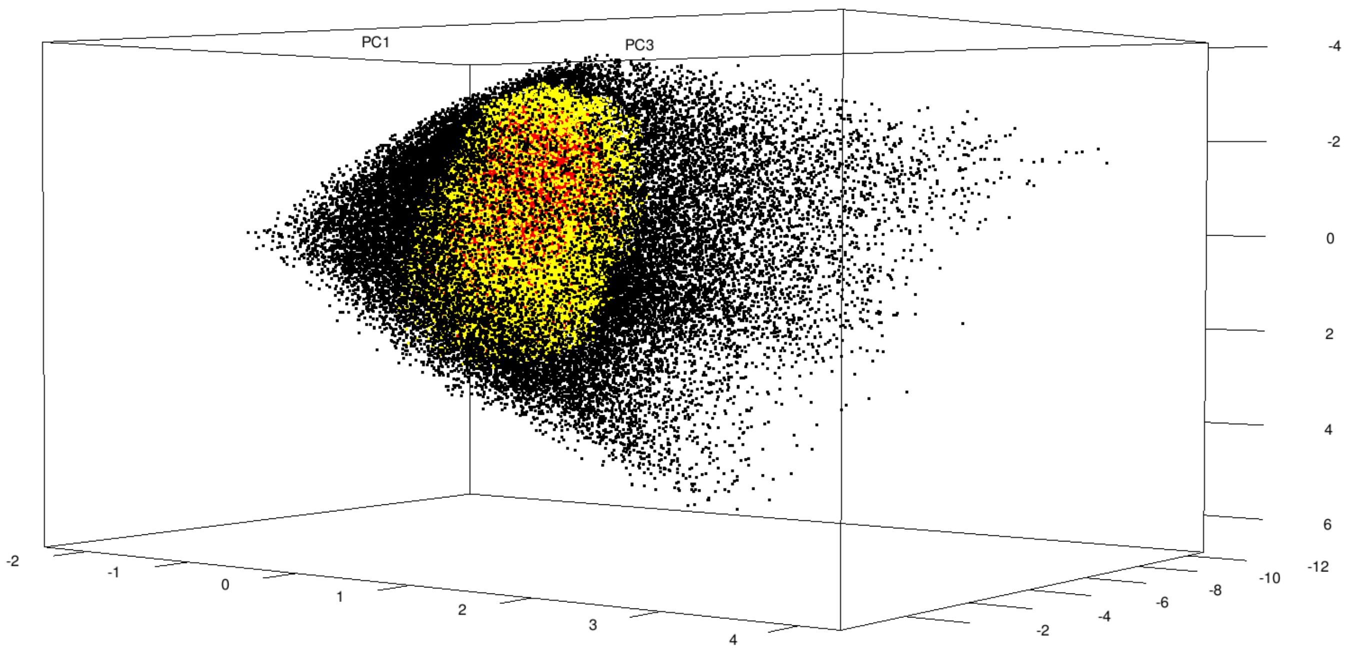

LUT reduction: using a singular value decomposition (SVD) of the correlation matrix of the measured and simulated spectral dataset

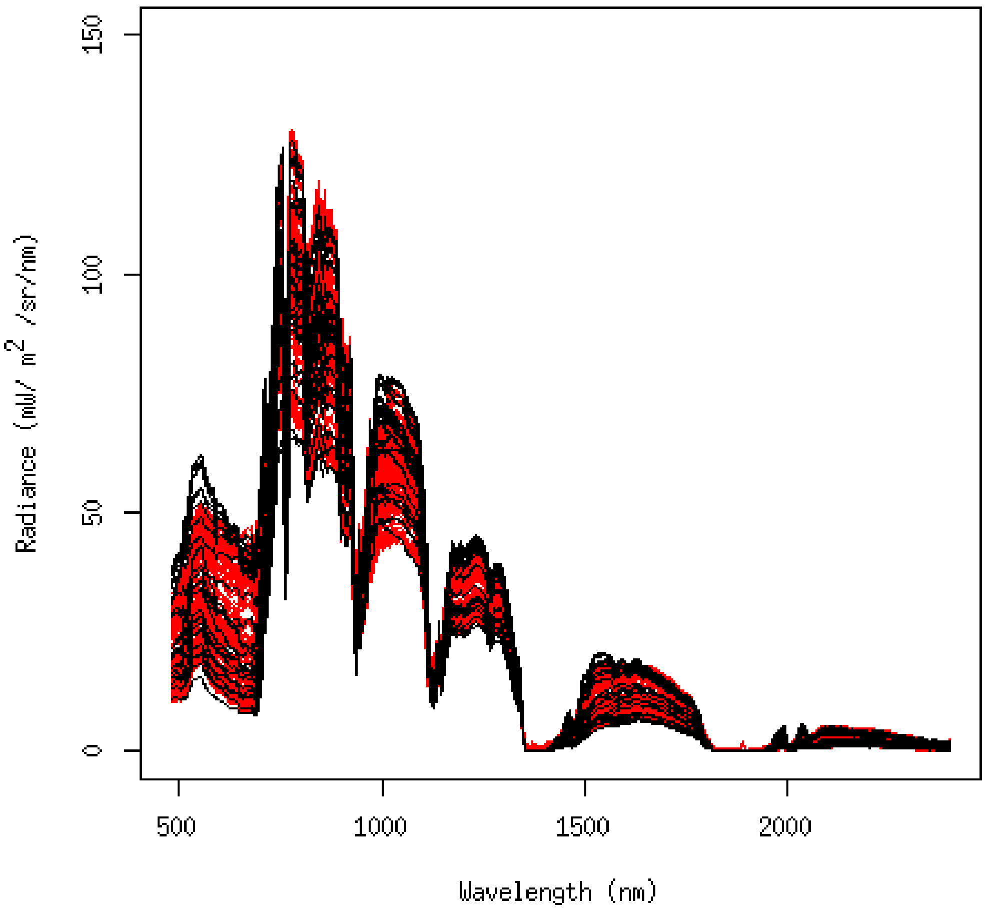

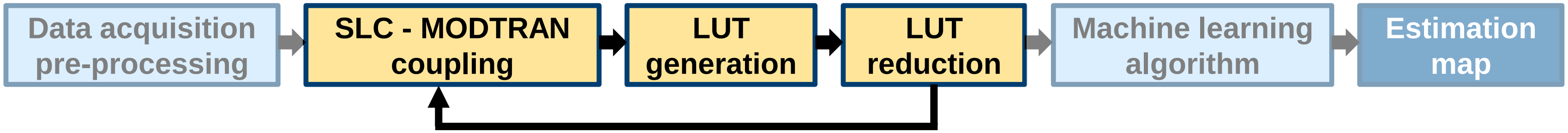

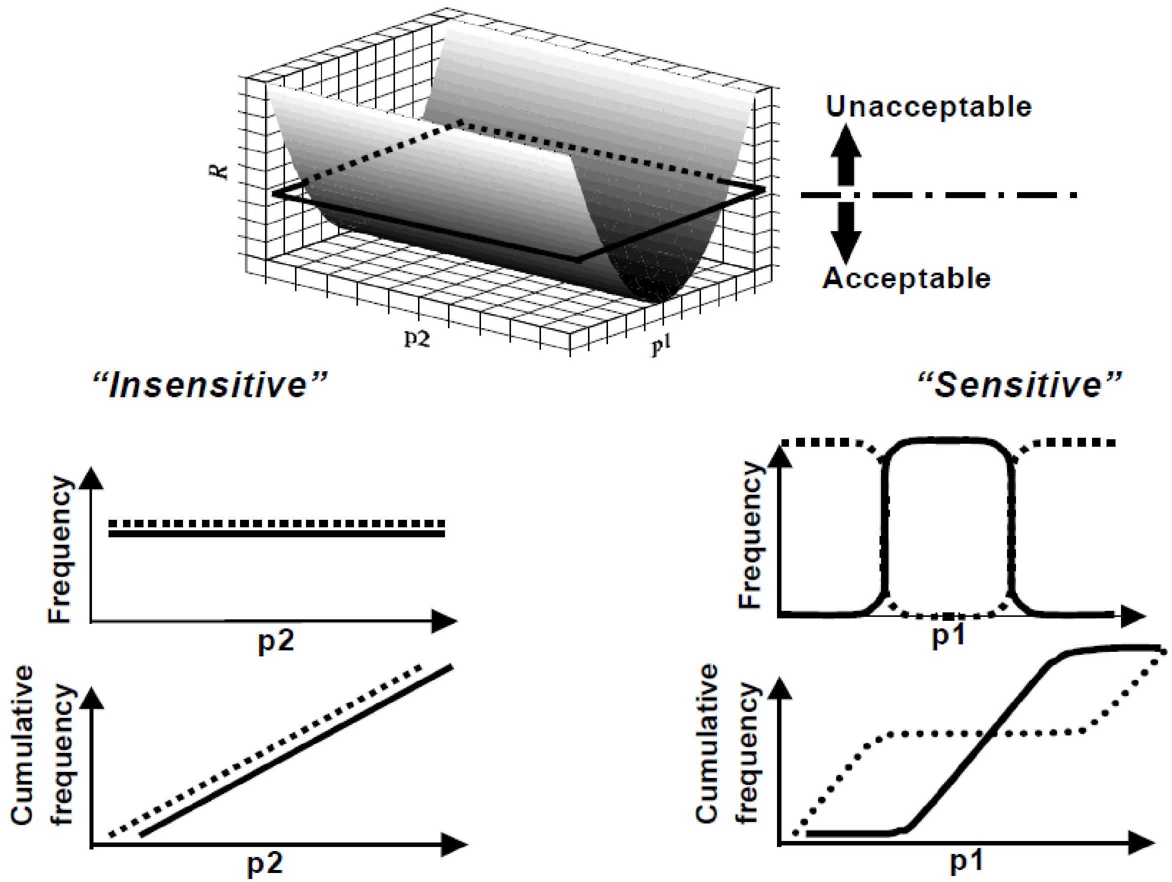

J. Choi, J. W. Harvey, and M. H. Conklin, "Use of multi-parameter sensitivity analysis to determine relative importance of factors influencing natural attenuation of mining contaminants," in *Proc. U.S. Geological Survey Toxic Substances Hydrology Program—Tech. Meet.*, vol. 1, Charleston, SC, Mar. 8–12, 1999, pp. 185–192.

Machine Learning algorithm

A support vector regression (SVR) was trained on the final reduced LUT

- Good generalization ability (+)
- Solves non-linear problems (+)
- Parameter tuning (-)

The regression model was used to predict LCC for each AISA pixel

$$f(x) = \sum_{i=1}^{\ell} \left(\alpha_i - \alpha_i^* \right) K(x_i, x) + b$$

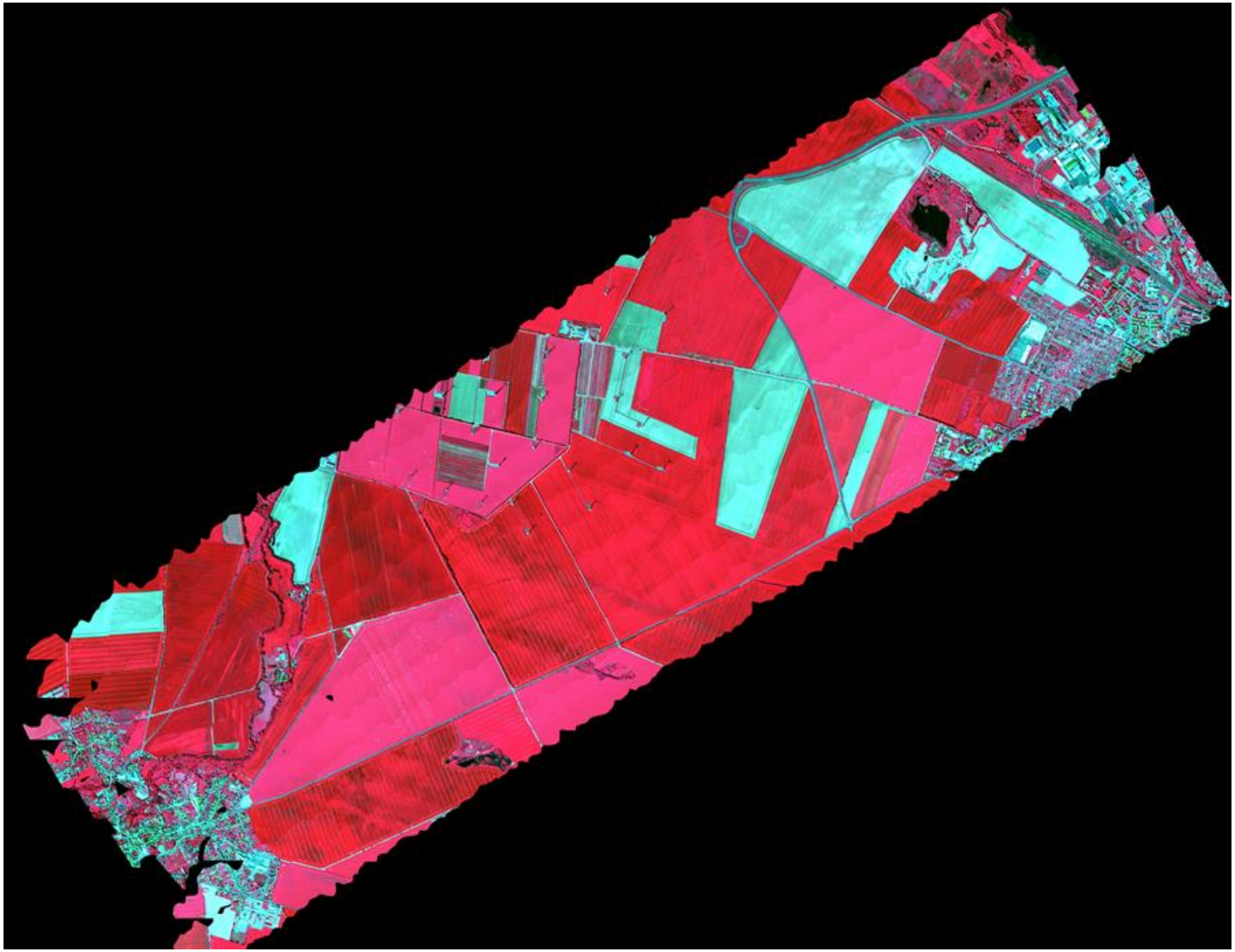

LAI estimation map

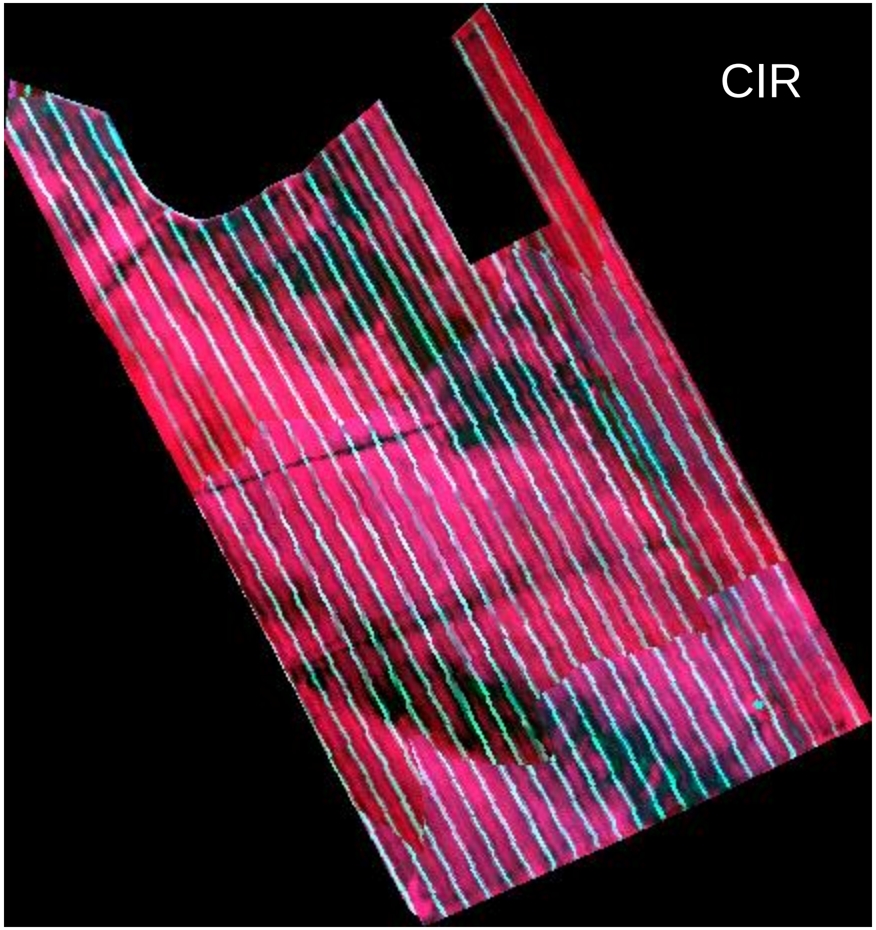

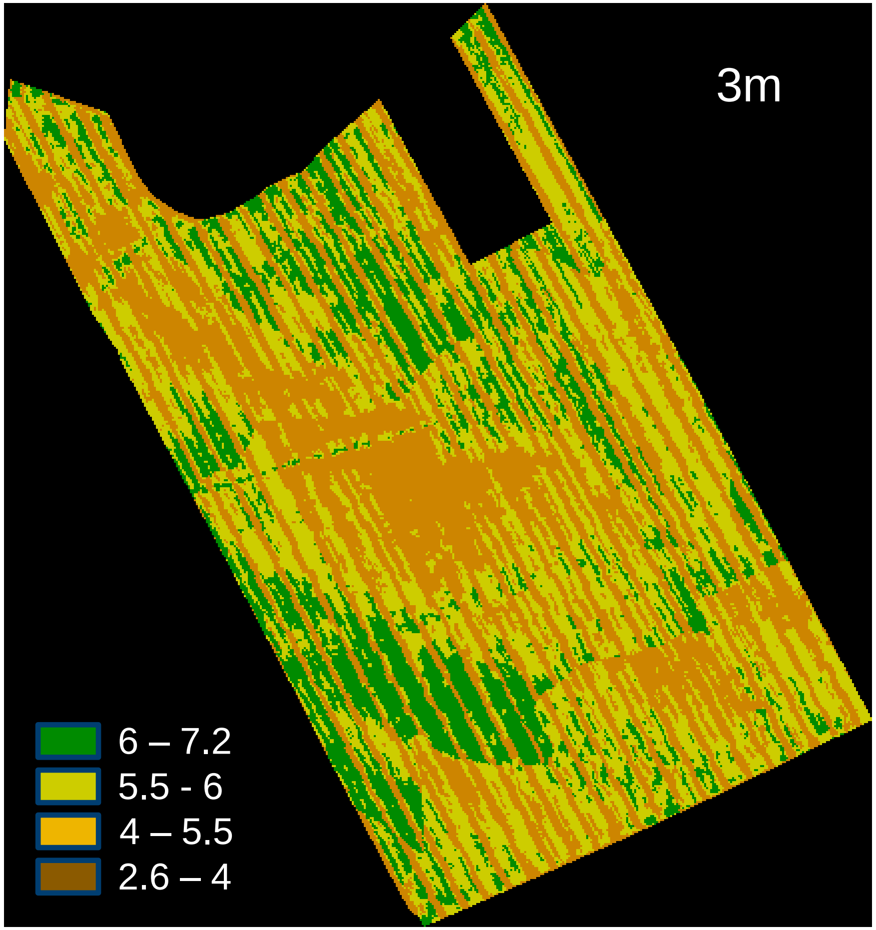

LAI estimation map

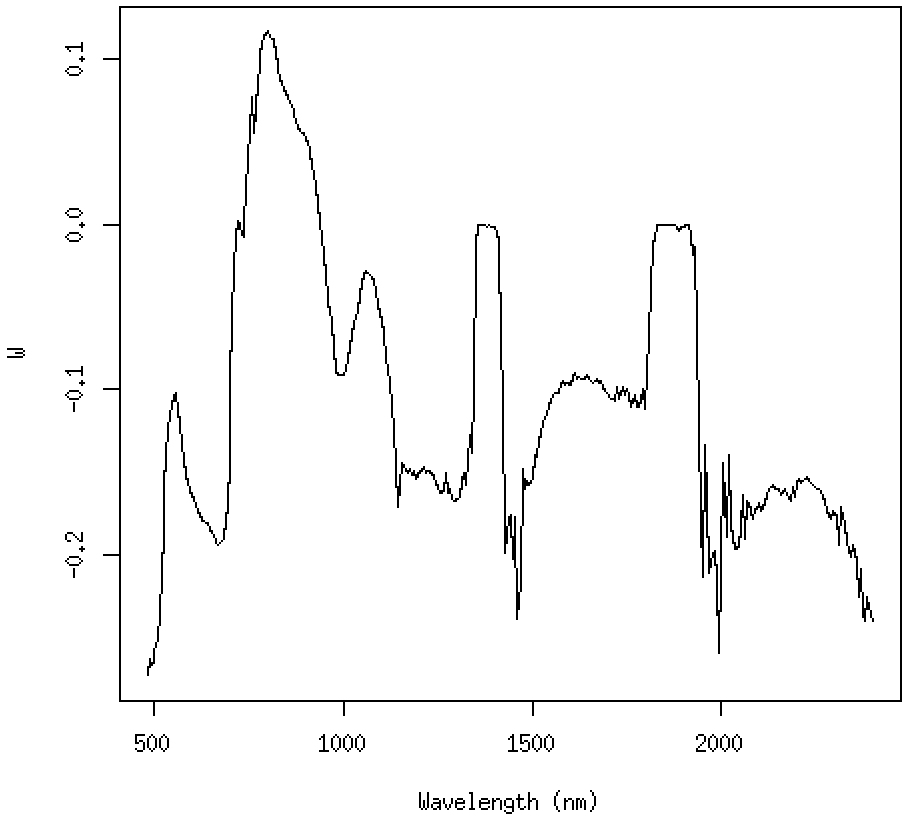

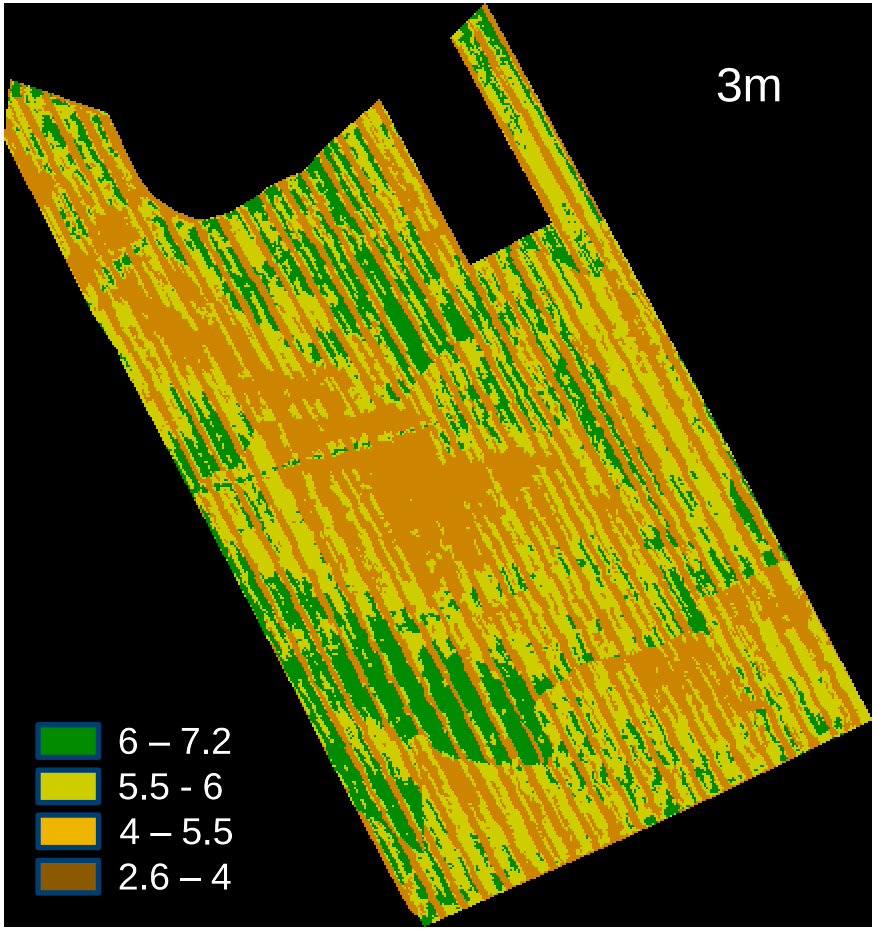

LAI estimation map

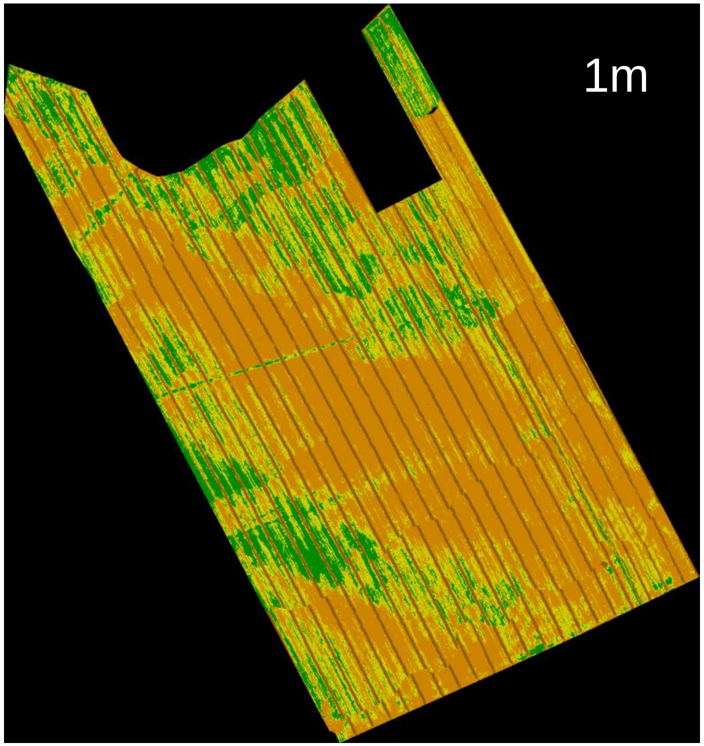

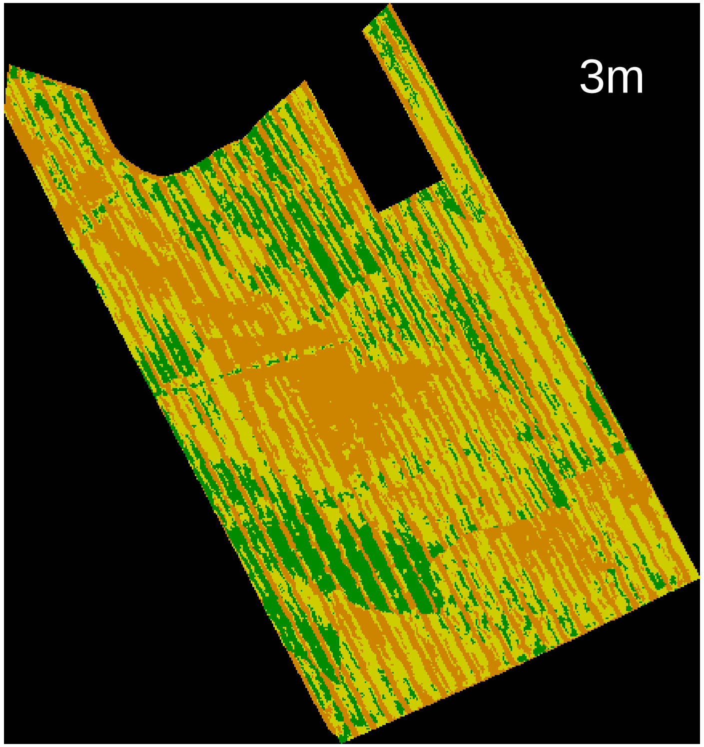

	Min	Max	Mean	SD
LICOR	3.2	7	5.4	1.3
1m	2.7	7.2	5.2	0.8
3m	4	7.2	5.5	0.6

- 6 – 7.2
- 5.5 - 6
- 4 – 5.5
- 2.6 – 4

	Min	Max
Cab	5	80
Cw	0.045	0.045
Cdm	0.0001	0.02
Cs	0.02	0.02
N	1	1.5
Cab	5	5
Cw	0.001	0.001
Cdm	0.005	0.005
Cs	0.8	0.8
N	2	2
LAI	0.5	8
LIDFu	-1	0
LIDFv	-1	0
hot	0.08	0.08
fB	0.03	0.03
Cv	0.85	0.85
zeta	0.45	0.45

Data acquisition pre-processing → **SLC - MODTRAN coupling** → **LUT generation** → **LUT reduction** → **Machine learning algorithm** → **Estimation map**

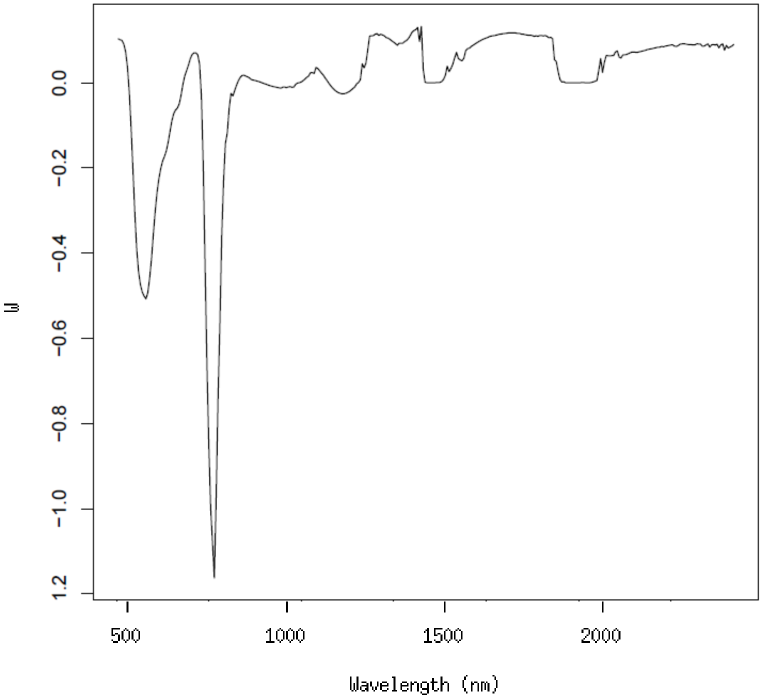

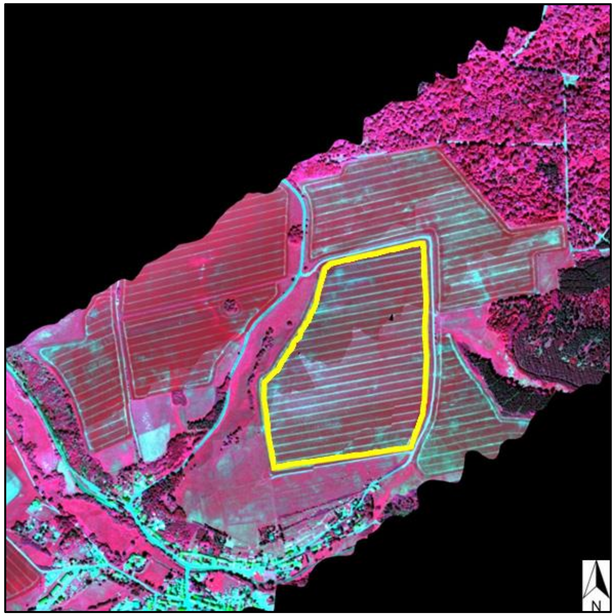

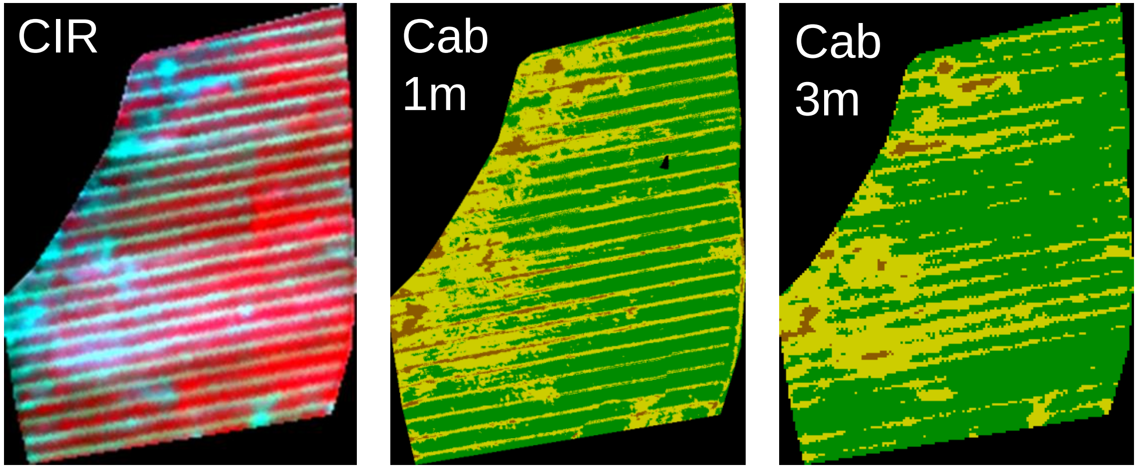

in µg cm^{-2}	Min	Max	Mean	SD
SPAD	35.6	52.3	44.2	4.6
1m	29.5	52.5	46.2	3.0
3m	33.9	52.7	47.3	2.5

- > 46 µg cm^{-2}
- 40-46 µg cm^{-2}
- < 40 µg cm^{-2}

Thank you for your attention!